The Pierce diode with an external circuit. I. Oscillations about nonuniform equilibria

William S. Lawson[a)]
Electronics Research Laboratory, University of California, Berkeley, California 94720

(Received 22 February 1988; accepted 28 March 1989)

The nonuniform (nonlinear) equilibria of the classical (short circuit) Pierce diode and the extended (series RLC external circuit) Pierce diode are described, and the spectrum of oscillations (stable and unstable) about these equilibria are worked out. It is found that only the external capacitance alters the equilibria, though all elements alter the spectrum. In particular, the introduction of an external capacitor destabilizes some equilibria that are marginally stable without the capacitor. Computer simulations are performed to test the theoretical predictions for the case of an external capacitor only. It is found that most equilibria are correctly predicted by theory, but that the continuous set of equilibria of the classical Pierce diode at Pierce parameters ($\alpha = \omega_p L/v_0$) that are multiples of 2π are not observed. This appears to be a failure of the simulation method under the rather singular conditions rather than a failure of the theory.

I. INTRODUCTION

The classical Pierce diode is perhaps the simplest of all theoretical models for a bounded plasma system. It was introduced by J. R. Pierce[1] to predict the maximum electron current that could be passed through a plasma device without instability. It consists of two parallel planes (plates or grids) and a cold electron beam traveling between them. The electrons are neutralized by a background population of infinitely massive ions. (In Pierce's model, this background was stationary, but for the purposes of this article it is better to think of them as comoving.) The planes are connected by a wire, and so are at the same potential. Pierce found that the behavior of the model was governed by the single parameter $\alpha = \omega_p L/v$, where ω_p is the plasma frequency of the electrons, L is the distance between the plates, and v is the velocity at which electrons enter the system. He also found that at the threshold value of $\alpha = \pi$ the device becomes unstable.

Since Pierce, the linearized behavior of this model has been studied in detail.[2,3] The linear modes as a function of α show a remarkable structure; between each multiple of π (excluding, of course, between zero and π), a mode goes from zero growth rate to some maximum, and back to zero. There are small ranges of values of α just below the odd multiples of π that are stable, but all other values of α greater than π lead to instability. The character of the unstable modes alternates between consecutive mutliples of π. For $2n\pi < \alpha < (2n+1)\pi$, the modes are oscillatory and growing, but for $(2n-1)\pi < \alpha < 2n\pi$, the modes are purely growing.

Godfrey[4] analyzed the nonlinear equilibria of the Pierce diode. He also discovered that the transition from instability to stability just below each odd multiple of π is a Hopf bifurcation and has a strange attractor associated with it.

The extended Pierce diode is similar to the standard (or classical) Pierce diode, but has passive circuit elements—any or all of a capacitor, a resistor, or an inductor in series—in place of the short circuit between the electrodes (see Fig. 1). This device is interesting as a second approximation to real bounded plasma systems. The linear behavior of this device has been worked out by Kuhn and Hörhager,[5] and verified by simulation.[6]

In this paper, the equilibria of the extended Pierce diode will be worked out, beginning with those derived by Godfrey. This task is greatly simplified by noting that the only type of circuit element that can alter an equilibrium is the capacitor. (The others can, of course, alter the *stability* of any given equilibrium.) The spectrum of linear oscillations about each of these equilibria will then be derived using the elegant integral equation formulation of the equations for the Pierce diode discovered by Godfrey.

At each step, computer simulations will be used to test and support the predictions of theory. Only in cases in which

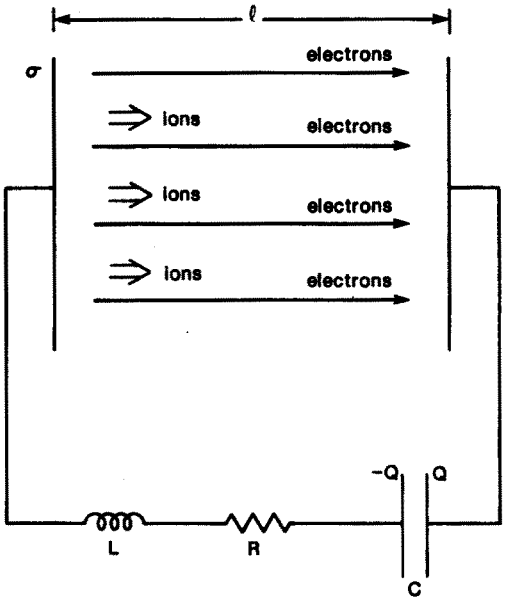

FIG. 1. Extended Pierce diode model.

[a)] Present address: Courant Institute of Mathematical Sciences, New York University, New York, NY 10012.

 0899-8221/89/071483-10$01.90

some singularity in the equations creates difficulty do the simulations fail to support the theory.

II. EQUILIBRIUM THEORY

The equilibrium equations are

$$\rho(x)v(x) = \rho_0 v_0, \tag{1}$$

$$v\frac{dv}{dx} = \frac{q}{m}E(x), \tag{2}$$

$$\frac{dE}{dx} = \frac{\rho - \rho_0}{\epsilon_0}, \tag{3}$$

with boundary conditions

$$\rho(0) = \rho_0, \tag{4}$$

$$v(0) = v_0, \tag{5}$$

$$\int_0^l E(x)dx = -V(E(0)), \tag{6}$$

where ρ, v, E, V, q/m, and ϵ_0 represent the electron charge density, electron velocity, electric field, potential drop across the diode, electron charge-to-mass ratio, and the dielectric constant of the vacuum. The first three of these are functions of the position x. The potential drop V may be a function of the electric field because of the external circuit element. For the classical Pierce diode, $V = 0$. The potential drop cannot depend on the time derivatives of the electric field, since the problem is a static one, but this implies that there can be no current flowing in the external circuit (unless one considers the constant injection flux of electrons to be balanced by an external current instead of an equal flux of massive ions). This in turn implies that *the external resistance or inductance will have no effect on the equilibria.* Only the capacitive case will produce new equilibria.

The equations can be made dimensionless by renormalizing as follows:

$$\alpha^2 = q\rho_0 l^2/\epsilon_0 m v_0^2 = (\omega_{p0} l/v_0)^2,$$

$$\rho' = \rho/\rho_0,$$

$$v' = v/v_0,$$

$$x' = x/l,$$

$$E' = (ql/mv_0^2)E,$$

$$V' = (q/mv_0^2)V.$$

Note that the charge of the electron has been absorbed into the electric field, so that the electric field is of the opposite sign as the physical electric field.

The resulting equations (dropping the primes) are

$$\rho v = 1, \tag{7}$$

$$v\frac{dv}{dx} = E, \tag{8}$$

$$\frac{dE}{dx} = \alpha^2(\rho - 1), \tag{9}$$

with the boundary conditions

$$\rho(0) = 1, \tag{10}$$

$$v(0) = 1, \tag{11}$$

$$\int_0^1 E(x)dx = -V(E(0)). \tag{12}$$

Although Godfrey gives the solution to these equations for the standard Pierce diode, he does not derive it. Since the solution is both simple and a good conceptual prelude to the solution of the time-dependent equations, here it is. Define t such that

$$\frac{dx}{dt} = v$$

and $t = 0$ at $x = 0$. This t represents the time it took a fluid element (or particle) to arrive at position x from its time of injection. It is not an independent variable in the usual sense, but rather a parameter of which both x and v will be functions. Equations (8) and (9) become

$$\frac{dv}{dt} = E, \tag{13}$$

$$\frac{dE}{dt} = \alpha^2(1 - v). \tag{14}$$

[Equation (7) was used to derive Eq. (14), and is now superfluous.] Either E or v may be eliminated to yield a harmonic oscillator equation. The solution, taking the boundary condition (11) into account is

$$E = E_0 \cos \alpha t, \tag{15}$$

$$v = 1 + (E_0/\alpha)\sin \alpha t, \tag{16}$$

$$x = t + (E_0/\alpha^2)(1 - \cos \alpha t). \tag{17}$$

The constant of integration E_0 represents the electric field at the injection plane, and may be either positive or negative.

A new condition is implicit in this solution; x must be a monotonically increasing function of t, so that $dx/dt = v$ must be greater than zero. Therefore, we must require that

$$1 + (E_0/\alpha)\sin \alpha t > 0 \tag{18}$$

for $0 < t < T$. For most cases, this will imply the condition $|E_0| < \alpha$. Note that since v is a single-valued function of t, the condition (18) is enough to ensure that v is a single-valued function of x, which is necessary for the fluid approximation to be valid.

The condition that v be single-valued is not at all restrictive, since all equilibria of interest must satisfy this condition anyway. When the system is in equilibrium, the total energy of an electron is constant and equal to $1/2mv^2 + q\phi$. Thus only two values of v are possible at any given position, implying that the electron trajectory can either go from the injection plane to the opposite plane without turning around at all, or it can turn around once and return to the injection plane. The case in which the electrons are turned around implies a large potential barrier, which cannot be created by the background ions, and cannot be sustained by a passive external circuit element in the face of the large ion current. Therefore, only the case in which v is a single-valued function of x is of interest.

Equation (17) applied at $x = 1$ gives an important relation between the time T that a particle or fluid element takes to transit the system, and E_0,

$$T = 1 - (E_0/\alpha^2)(1 - \cos \alpha T). \tag{19}$$

The second boundary condition, Eq. (12), can now be applied. The new boundary condition involves the potential drop across the system,

$$-V(E)=\int_0^1 E\,dx$$

$$=\int_0^T E\frac{dx}{dt}dt$$

$$=\int_0^T E_0\cos\alpha t\left(1+\frac{E_0}{\alpha}\sin\alpha t\right)dt$$

$$-V(E)=\frac{E_0}{\alpha}\sin\alpha T\left(1+\frac{E_0}{2\alpha}\sin\alpha T\right). \tag{20}$$

A. Equilibria without a capacitor

Let us first consider the classical Pierce diode. In this case, $V(E)=0$, so

$$E_0=0, \tag{21}$$

or

$$\sin\alpha T=0, \tag{22}$$

or

$$[1+(E_0/2_\alpha)\sin\alpha T]=0. \tag{23}$$

The first case (21) is the uniform equilibrium, and the third case (23) implies that $v(1)=-1$, which violates the condition that the velocity be positive, so the second case (22) is the interesting one. The solution is simply

$$T=\pi n/\alpha. \tag{24}$$

Putting this into Eq. (19) yields two results depending on whether n is even or odd. If n is even,

$$\alpha=n\pi \tag{25}$$

and E_0 is unconstrained [except for condition (18)]. If n is odd,

$$E_0=(\alpha/2)(\alpha-n\pi). \tag{26}$$

The condition that the velocity be positive requires (except for $n=1$ when $E_0>0$) that $|E_0|/\alpha<1$. For any given n this condition limits the range of α over which a valid solution exists. The case $n=1$ is different for $E_0>0$, since $\sin\alpha t$ is always positive in this case. Thus for $n=1$, there is no upper bound on E_0. This equilibrium structure can be diagrammed as in Godfrey (Fig. 3 of Ref. 4) (see Fig. 2). The stability of these modes wlll be considered later, but the equilibria with $E_0<0$ are, in fact, unstable, while those with $E_0>0$ are stable. If the initial value of the electric field at the injection plane is slightly less negative than the value E_0 for an unstable equilibrium, then the system will decay either to the uniform equilibrium (if the uniform equilibrium is stable), or to an oscillating state. If E_0 is more negative than the equilibrium value, then the growth of the unstable mode leads to virtual cathode formation.

B. Equilibria with a capacitor

When the external circuit contains a capacitor, the equations become more complicated. First, let us derive the proper expression for $V(E_0)$ [recall that $E_0=E(0)$]. The voltage across the capacitor is

$$V=Q/C,$$

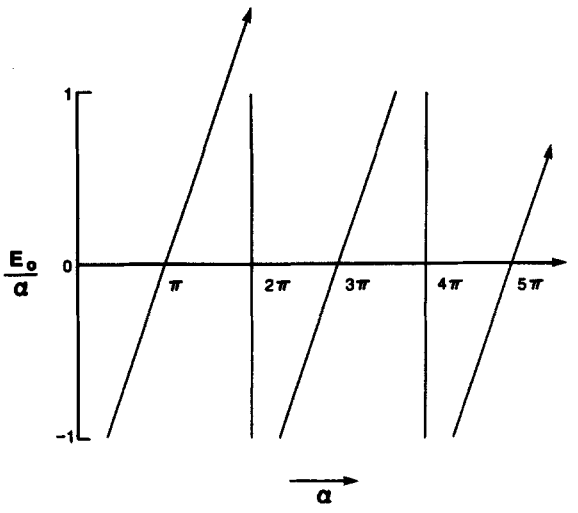

FIG. 2. Nonuniform equilibria for short circuit ($C=\infty$) case. All lines end at $|E_0|=\alpha$ except for first line (with arrow), which extends indefinitely.

where the sign of Q is chosen as in Fig. 1. The total surface charge on the injection plane must be $\sigma=Q/A$ (where A is the area of the injection plane) if the unperturbed state $E_0=V=0$ is to be accessible. This surface charge gives rise to the electric field at the injection plane, E_0, such that

$$E_0=\sigma/\epsilon_0.$$

Putting all this together,

$$V(E_0)=(\epsilon_0 A/C)E_0. \tag{27}$$

Converting to normalized units gives

$$V'(E_0')=(\epsilon_0 A/lC)E_0',$$

$$=(C_0/C)E_0',$$

where C_0 is the vacuum capacitance between the injection and collection planes. Thus, defining

$$C'=C/C_0$$

yields the dimensionless equation (again dropping the primes)

$$V=E_0/C. \tag{28}$$

Equation (20) now becomes

$$\frac{E_0}{\alpha}\sin\alpha T\cdot\left(1+\frac{E_0}{2\alpha}\sin\alpha T\right)=-\frac{E_0}{C}. \tag{29}$$

This equation can be solved parametrically by setting a phase variable $\phi=\alpha T$ and combining it with Eq. (19). The result is

$$\alpha=\frac{[\frac{1}{2}\phi\sin^2\phi-\sin\phi(1-\cos\phi)]}{[\frac{1}{2}\sin^2\phi+(1-\cos\phi)/C]}, \tag{30}$$

$$\frac{E_0}{\alpha}=-\frac{(\sin\phi+\phi/C)}{[\frac{1}{2}\sin^2\phi+(1-\cos\phi)/C]} \tag{31}$$

Figure 3 shows several diagrams like Fig. 2 that give the equilibrium values of E_0 as a function of α for various values of C. For finite values of the capacitor, it can be seen that the modes which were at $\alpha=2n\pi$ merge with the modes which are at the next smallest value of α. For large values of C and small values of α, this merging occurs at values of E_0 that

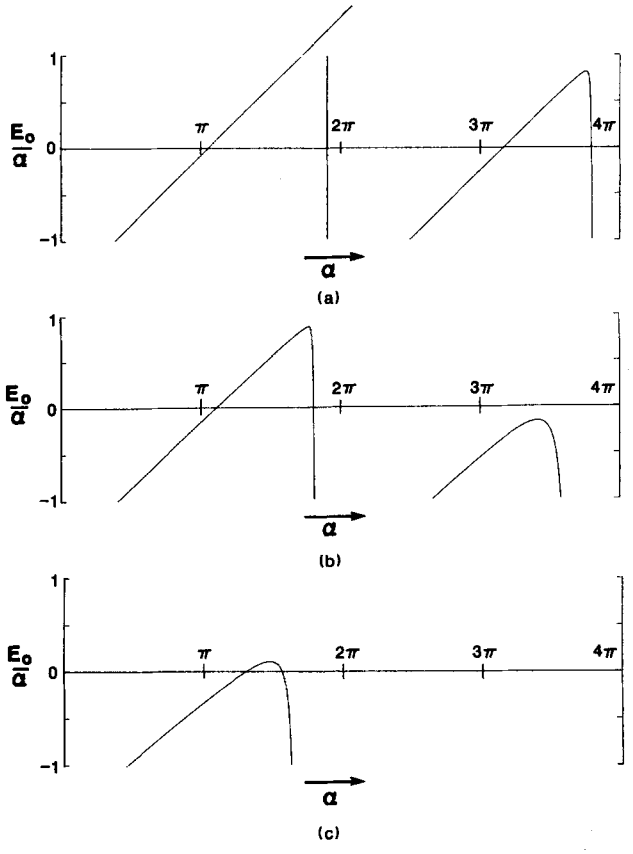

FIG. 3. Nonuniform equilibria for (a) $C = 20$, (b) $C = 10$, and (c) $C = 5$. Note that in (a), the first line does not go on indefinitely, but ends as shown.

exceed the constraint (18), and so are not seen in the graphs. Note that the $n = 1$ mode, which existed for arbitrarily large values of α when C was infinite, ends, as shown in Fig. 3(a), at a finite value of α.

Some interesting points can be shown analytically; for instance, at the points at which there are bifurcations with the uniform equilibrium (i.e., when $E_0 \to 0$), Eq. (29) reduces to

$$\sin\alpha = -\alpha/C \tag{32}$$

(since $E_0 = 0$ implies $T = 1$). These are the values of α at which the uniform equilibrium goes from stable to unstable behavior. Note that this equation has only a *finite* number of roots, implying that beyond a certain value of α (for a given C), there are no more bifurcations, i.e., beyond $\alpha = C$, there can be no stable equilibria except (possibly) the uniform equilibrium. The curves for E_0 seem to drop off the graph as the value of C decreases, so one can also look for a criterion for which there are no equilibria at all other than the uniform equilibrium. Again using Eq. (29) with $E_0 = -\alpha$, there can be solutions only if $\alpha < 3/2C$.

The different branches of the curves in Fig. 3 correspond to ranges of ϕ that are bounded below by an odd multiple of π and above by an even multiple of π. Other ranges of ϕ yield a very negative E_0. As might be expected, as $C \to \infty$, the sloping part of each branch corresponds to ϕ near to the odd multiple of π, and the part of the branch that is approaching vertical corresponds to ϕ near to the even multiple of π. It is useful to note that at $\phi = \pi$, the limit of E/α is $-\pi/2$, regardless of the value of C. While this solution at $\alpha = 0$ is of no interest physically, since it violates condition (18), it does constrain the first branch of the curve.

TABLE I. Simulation parameters. Units are arbitrary but self-consistent.

System length	1
Number of grid cells	128
Time step	1/128
Number of time steps	2048
ϵ_0	1
q_e/m_e	-1
m_i	∞
v_0	1
Injected electron current	$-\alpha^2$
Background current	α^2
Injected electron flux	2048

III. SIMULATION RESULTS FOR EQUILIBRIA

The particle simulation code PDW1[7] was used to simulate the expected equilibria. As with the theory, the simulation results will be broken up into the classical (short circuit) and extended (capacitive external circuit) cases. The simulation parameters are shown in Table I.

A. Classical Pierce diode

The easiest equilibria to simulate are the stable ones. To simulate these, the uniform equilibrium was given a slight perturbation, and the equilibria came about naturally. Figures 4 and 5 show the phase space plots after equilibrium has been reached and time histories of the electric field at $x = 0$ as the simulation approaches equilibrium for α equal to $3\pi/2$, $7\pi/2$, and $11\pi/2$. These equilibria were observed by Crystal and Kuhn,[3] although they did not compare them with theory. While in all three cases the electric field at $x = 0$ settles down rapidly to the average value predicted by Eq. (26), the results are not without surprises. The electric field at $x = 0$ for both $\alpha = 7\pi/2$ and $\alpha = 11\pi/2$ shows oscillations about the equilibrium value that are only weakly damped. These oscillations will be examined when the general issue of stability is addressed.

The stable equilibrium with $n = 1$ extends to all values of $\alpha > \pi - 2$. This can also be simulated in regions where

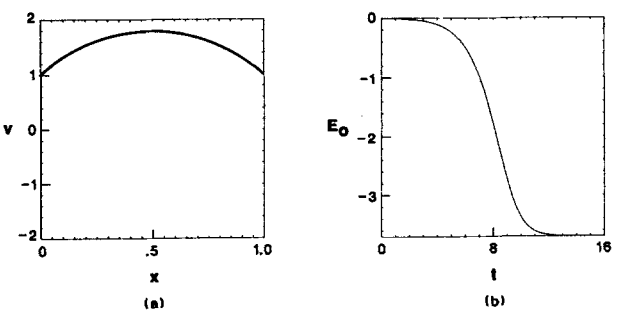

FIG. 4. Phase space at the end of the run and the history of E_0 for the short circuit case with $\alpha = 3\pi/2$. (Phase space plot is actually comprised of many particles, and not a single curve, as it appears.)

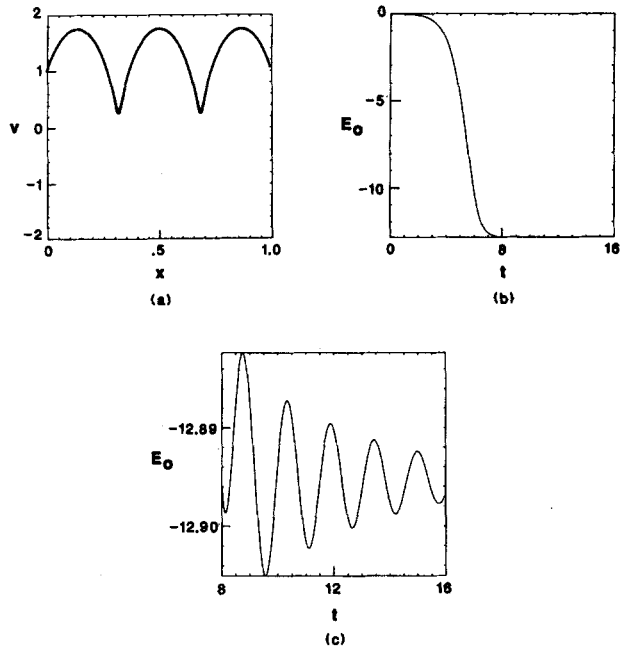

FIG. 5. Phase space at the end of the run and the history of E_0 for the short circuit case with $\alpha = 11\pi/2$. [Figure (c) is a blow-up of the last half of Fig. (b).]

other equilibria are preferred, such as $\alpha = 5\pi/2$. To do this, it is not enough to perturb the uniform equilibrium, since this perturbation will not grow to the desired equilibrium. Instead, the electric field at the injection plane E_0 is held fixed at the predicted equilibrium value, overriding the circuit condition for one transit time. This constraint should force the desired equilibrium. After a transit time (or more), the constraint can be removed, and the self-consistent circuit condition reinstated. When this is done for $\alpha = 5\pi/2$, forcing $n = 1$, the predicted equilibrium is found, with no oscillations about the equilibrium value of E_0. Table II summarizes the results for the stable equilibria. The values for $\alpha = 3\pi/2$ and $\alpha = 5\pi/2$ are extraordinarily accurate, but the values for $\alpha = 7\pi/2$ and $\alpha = 11\pi/2$ seem to deviate significantly. Halving the grid spacing and the time step reduced the error for $\alpha = 11\pi/2$ from 5% to 1.5%, and Richardson extrapolation assuming second-order accuracy reduces this to 0.5%, so it appears that the deviation is of numerical rather than physical origin.

The unstable equilibria are rather difficult to simulate. One approach is to again fix E_0, overriding the circuit constraint, at a value either above or below the predicted equilibrium value of E_0 for a transit time, then restore the circuit constraint and see whether the simulation moves away from the predicted equilibrium. This was done for the $\alpha = \pi/2$ equilibrium. The predicted value for E_0 in equilibrium is $E_0 = -\pi^2/8 \approx -1.23$, so two simulations were run at initial values of E_0 at -1.2 and -1.3 (recall that the sign of E_0 is different in the theory from the simulations with negatively charged electrons). The results of the simulation starting at $E_0 = -1.2$ are not shown, but the system quickly settles to the stable uniform equilibrium ($E_0 = 0$, $v = 1$). When $E_0 = -1.3$, however, a virtual cathode forms (see Fig. 6). If any physical quantity (here the electrostatic energy) is plotted versus time, it is seen that a very regular, though nonsinusoidal, virtual cathode oscillation has set in (see Fig. 7). Recall that this oscillation occurs at a value of α that is only half of the value at which the Pierce diode first becomes linearly unstable (1/4 the current).

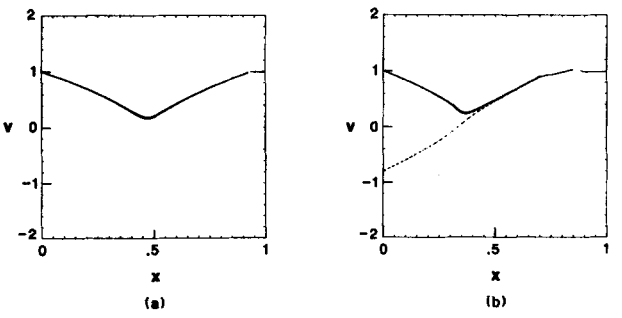

FIG. 6. Early (a) and late (b) phase space plots for the short circuit case with an initial $E_0 = -1.3$.

The unstable equilibrium at $\alpha = 5\pi/2$ was also simulated. The results are shown in Fig. 8. Since no regular virtual cathode oscillations were expected (and none were found), E_0 was again fixed for a transit time, this time at exactly the value predicted for the equilibrium. There are two pieces of evidence that the predicted equilibrium exists at very nearly the predicted value of E_0. First, the potential returns almost to zero at $x = 1$, and second, when released, the growth away from the equilibrium appears to be exponential rather than linear. The equilibrium is marred by the presence of two trapped electrons (just visible near $x = 0.75$ and $x = 0.85$, slightly below the passing electrons). According to continuum theory, these trapped particles should not be there, but the errors inherent in simulation allow them to become trapped during the initial transient (the diode is initially in

TABLE II. Equilibria for a classical Pierce diode. Values of the electric field at the cathode for different values of α.

α	E_0 theory	E_0 simulation
$3\pi/2$	$-3.701\,10$	-3.7009
$5\pi/2$	$-18.505\,51$	-18.5061
$7\pi/2$	$-8.635\,90$	-8.528
$11\pi/2$	$-13.570\,71$	-12.895
		$(-13.357)^a$

[a] Δx and Δt reduced by half.

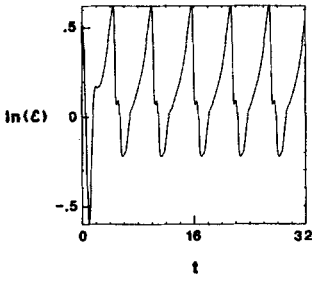

FIG. 7. Virtual cathode oscillations in the stable region with initial $E_0 = -1.3$. Here, $\mathscr{E}$ represents the total electrostatic energy.

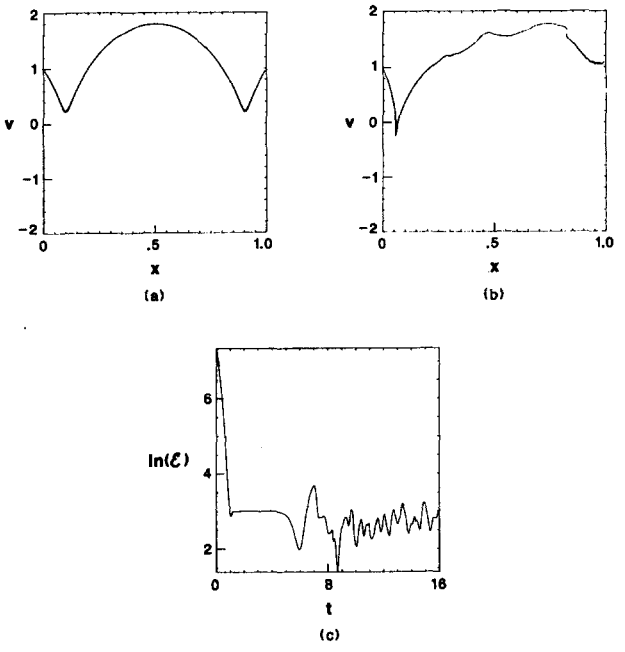

FIG. 8. Early (a) and late (b) phase space plots and the history (c) of E_0 for unstable equilibrium in the short circuit case with $\alpha = 5\pi/2$. Again, $\mathscr{E}$ represents the total electrostatic energy.

the uniform state). If these particles were not there, the agreement might be even better.

The equilibria at $\alpha = 2n\pi$ are especially interesting because any value of E_0 that does not violate condition (18) should be a valid equilibrium. Trouble can be expected, however, since the dispersion relation of the uniform equilibrium has a double root of zero at $\alpha = 2n\pi$, implying a secular instability (linear growth with time). This secular instability may (and the section on stability will show shortly that it does) extend to the nonuniform equilibria. This secular instability is of interest, but simulation efforts have not met with success. Particle simulation at $\alpha = 2\pi$ produces a slowly but exponentially growing mode, and a simulation based on Godfrey's integral equation formulation produces a mode that oscillates slowly about the uniform equilibrium with large amplitude. The reason for the failure of these simulations seems to be the singular nature of the $\alpha = 2n\pi$ points. For values of α near these points, the dominant solution of the dispersion relation varies as $\theta \sim (2n\pi - \alpha)^{1/2}$. Thus a very small numerical error can produce relatively large deviations. For instance, an error that alters the effective value of α by 1/1000 may create a growth rate or frequency of 1/30, which is quite noticeable in simulation.

TABLE III. Equilibria for an extended Pierce diode. Values of the electric field at the cathode for different values of α and C.

C	E_0 theory	E_0 simulation	α
20	−3.1399	−3.1398	$3\pi/2$
10	−2.5306	−2.5306	$3\pi/2$
5	−0.4863	−0.4885	$3\pi/2$
20	−5.3689	−5.336	$7\pi/2$

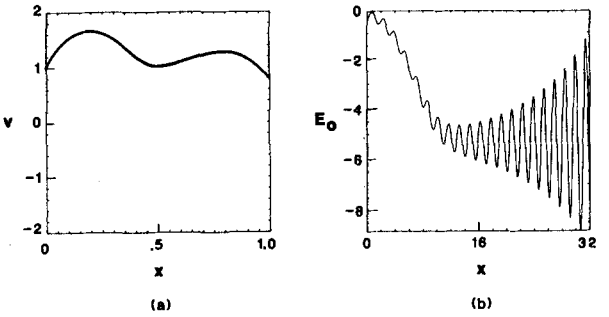

FIG. 9. Phase space plot and history of E_0 for the almost-stable mode at $\alpha = 7\pi/2$ with $C = 20$.

B. Equilibria with external capacitor

To test the predictions for the equilibria with an external capacitor, α was again chosen to be half-integer multiples of π in the simulations. The results for the stable equilibria are in Table III. The results are very good for $\alpha = 3\pi/2$, and somewhat less good for $\alpha = 7\pi/2$. As was demonstrated for the short circuit case, this less-accurate agreement is most likely due to the error inherent in the simulation, since the time step is larger relative to a plasma period (i.e., $\omega_p \Delta t$ is larger).

Interestingly, the equilibrium for $\alpha = 7\pi/2$ and $C = 20$ is not truly stable. There is an oscillatory mode that has a small but unmistakable growth rate (see Fig. 9). This growth will be explained in the next section.

The unstable equilibrium at $\alpha = 7\pi/2$ and $C = 10$ was also simulated, and the phase space plot is shown in Fig. 10. The growth rate for this mode is quite slow relative to the short circuit case.

IV. STABILITY OF NONUNIFORM EQUILIBRIA

The most direct method of analyzing the stability of an equilibrium is to compute the spectrum of linear perturbations about that equilibrium. Fortunately, this is possible for the extended Pierce diode. One simple method of doing this is to extend the set of integral equations discovered by Godfrey for the classical Pierce diode. Godfrey's integral formu-

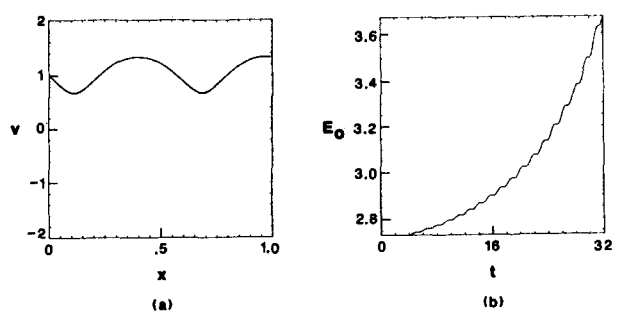

FIG. 10. Phase space plot and history of E_0 for the almost-stable mode at $\alpha = 7\pi/2$ with $C = 10$ and initial E_0 near the equilibrium value.

lation of the Pierce diode, extended to the case with an external circuit, is comprised of the two integrodifferential equations

$$T(t) - 1 = -\frac{1}{\alpha}\int_{t-T}^{t} E(\tau)\sin\alpha(t-\tau)d\tau \tag{33}$$

and

$$\left(L\frac{d^2}{dt^2} + R\frac{d}{dt} + \frac{1}{C} + 1\right)E(t) = \frac{\alpha^2}{2}[1 - T(t)^2] - \alpha\int_{t-T}^{t} E(\tau)(t-\tau) \times \sin\alpha(t-\tau)d\tau, \tag{34}$$

where x and t represent position and time, respectively, E represents the electric field at the injection plane, T represents the transit time of the electron just leaving the system, α is the classical Pierce parameter, and R, L, and C represent the external resistance, inductance, and capacitance. All these quantities have been normalized as before, with the additional normalizations

$$C' = C/C_0,$$
$$R' = (v_0/l)RC_0,$$
$$L' = (v_0^2/l^2)LC_0,$$

where $C_0 = \epsilon_0 A/l$, as before. [The derivation of Eqs. (33) and (34) is little different from that given by Godfrey,[6] and will not be given here. It hinges on the derivation and solution of the equation $\ddot{v} + \alpha^2 v = \partial E_0/\partial t + \alpha^2$, which is a relative of the Llewelyn equation $\ddot{v} = J$ used in vacuum tube theory—see Llewelyn[8].]

These equations are idealy suited to linearization about nonuniform equilibria.

A. Linearization about an equilibrium

Assume that $E = E_0$, $T = T_0$ is a solution of (33) and (34) for some given α and C, then (33) and (34) can be linearized:

$$\delta T = -\frac{1}{\alpha}\int_{t-T}^{t}\delta E(\tau)\sin\alpha(t-\tau)d\tau - \frac{1}{\alpha}\int_{t-T}^{t-T_0} E_0\sin\alpha(t-\tau)d\tau$$
$$\approx -\frac{1}{\alpha}\int_{t-T_0}^{t}\delta E(\tau)\sin\alpha(t-\tau)d\tau - \frac{E_0}{\alpha}\sin\alpha T_0\,\delta T,$$

so

$$\left(1 + \frac{E_0}{\alpha}\sin\alpha T_0\right)\delta T = -\frac{1}{\alpha}\int_{t-T_0}^{t}\delta E(\tau)\sin\alpha(t-\tau)d\tau. \tag{35}$$

The equation for $E(t)$ can be similarly linearized.

$$\left(L\frac{d^2}{dt^2} + R\frac{d}{dt} + \frac{1}{C} + 1\right)\delta E = -\alpha^2 T_0\,\delta T - \frac{\alpha^2}{2}(\delta T)^2 - \alpha\int_{t-T}^{t}\delta E(\tau)(t-\tau)\sin\alpha(t-\tau)d\tau - \alpha\int_{t-T}^{t-T_0} E_0(t-\tau)\sin\alpha(t-\tau)d\tau$$
$$\approx -\alpha^2 T_0\left(1 + \frac{E_0}{\alpha}\sin\alpha T_0\right)\delta T - \alpha\int_{t-T_0}^{t}\delta E(\tau)(t-\tau)\sin\alpha(t-\tau)d\tau.$$

Substituting in (35),

$$\left(L\frac{d^2}{dt^2} + R\frac{d}{dt} + \frac{1}{C} + 1\right)\delta E = \alpha\int_{t-T_0}^{t}\delta E(\tau)(T_0 - t + \tau)\sin\alpha(t-\tau)d\tau = \alpha\int_{0}^{T_0}\delta E(t-t')(T_0-t')\sin\alpha t'dt'. \tag{36}$$

Both sides of (36) are linear in δE, so a solution of the form $\delta E = \exp(\theta t)$ can be sought. When this form for δE is substituted into (36), the result is

$$L\theta^2 + R\theta + \frac{1}{C} + 1 = \alpha\int_0^{T_0} e^{-\theta t'}(T_0 - t')\sin t'dt' = \frac{\alpha^2 T_0}{\alpha^2+\theta^2} - \frac{\alpha}{(\alpha^2+\theta^2)^2}[2\alpha\theta(1 - e^{-T_0\theta}\cos\alpha T_0) + (\alpha^2 - \theta^2)e^{-T_0\theta}\sin\alpha T_0]. \tag{37}$$

Note that this equation does not contain E_0.

This formula (without the external circuit elements) was first published by Godfrey [his Eq. (23)], although he did not publish its derivation, nor did he make use of it. This formula can now be applied to some special cases of interest.

B. Uniform equilibrium

In the uniform ($E = 0$ for all x) equilibrium $T_0 = 1$, so

$$L\theta^2 + R\theta + \frac{1}{C} + \frac{\theta^2}{\alpha^2+\theta^2} + \frac{\alpha}{(\alpha^2+\theta^2)^2} \times [2\alpha\theta(1 - e^{-\theta}\cos\alpha) + (\alpha^2 - \theta^2)e^{-\theta}\sin\alpha] = 0. \tag{38}$$

This is the dispersion relation found by Kuhn and Hörhager.[5]

C. Nonuniform equilibrium with short circuit

As Godfrey showed, the nonuniform equilibria when the external circuit is a short (classical Pierce diode) are of

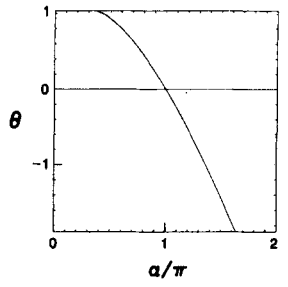

FIG. 11. Dispersion curve for the dominant mode of 2 nonuniform equilibrium in the short circuit case for $0<\alpha<2\pi$ (Im θ is zero for this mode).

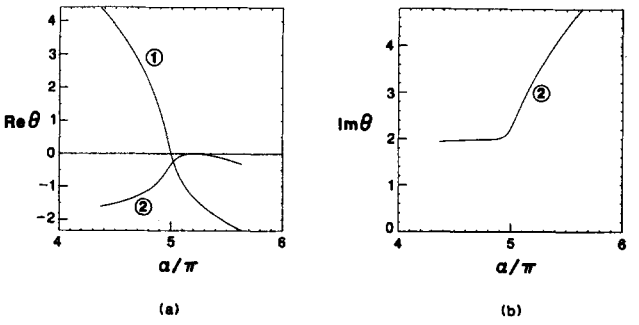

FIG. 13. Dispersion curves for dominant modes of a nonuniform equilibrium in the short circuit case for $4\pi<\alpha<6\pi$. The mode that is dominant for $\alpha/\pi<5$ is purely growing.

two classes depending on whether an integer parameter n is odd or even. When n is even, the equilibrium is given by $\alpha=n\pi$, $T_0=1$, and E_0 with any value as long as $-\alpha<E_0<\alpha$ [as per Eq. (25)]. Putting these values into (37) with $L=R=1/C=0$ gives

$$\frac{\theta^2}{n^2\pi^2+\theta^2}+\frac{2n^2\pi^2\theta}{(n^2\pi^2+\theta^2)^2}(1-e^{-\theta})=0. \tag{39}$$

Note that the same dispersion equation applies for all values of E_0. The dominant root of this equation is $\theta=0$, which is a double root, implying that a secular instability is possible. As was mentioned, this secular instability was not observed in simulations, and the singular behavior near $\alpha=n\pi$ with n even seems to be responsible for the poor simulation results.

When n is odd, $T_0=n\pi/\alpha$, and $E_0=\frac{1}{2}\alpha(\alpha-n\pi)$. Substituting these values into (32) gives

$$1-\frac{n\pi\alpha}{\alpha^2+\theta^2}+\frac{2\alpha^2\theta}{(\alpha^2+\theta^2)^2}\left[1+\exp\left(-\frac{n\pi}{\alpha}\theta\right)\right]=0. \tag{40}$$

Figures 11–13 show the dominant solutions of this dispersion relation as a function of α for the regions of interest $(n\pi-2<\alpha<n\pi+2)$ for $n=1,3,5$. For $n\pi-2<\alpha<n\pi$, the dominant mode is purely growing in all cases. For $n\pi<\alpha<n\pi+2$, the dominant mode is always purely damped for $n=1$, but for $n>1$ a second mode, which is damped and oscillatory, appears, and seems to touch Re $\theta=0$. This is not an illusion, and the values of α at which the real part of the eigenvalue θ is zero can be found by setting $\theta=i\omega$ and setting the real and imaginary parts of (40) to zero. The result is a Diophantine equation,

$$\alpha/\pi-n=nm^2/(n^2-m^2), \tag{41}$$

in which m must be odd. Only values of $\alpha/\pi-n$ between $-2/\pi$ and $2/\pi$ are of interest. In this region, one quickly finds that

$$n>(\pi/2+1/n)m^2$$

is a necessary condition. From this it is plain that for $n=1$, no such solutions are expected, and for $n=3$ and $n=5$, one such solution is expected. Two solution will not appear until $n=15$.

The simulations from the previous article agree with the predictions of this dispersion relation as well as can be determined from the graphs (the eigenvalues were not computed numerically from the simulations).

The case in which θ is purely imaginary is of special interest, since any growth or decay must be determined by nonlinear effects. Figure 14 shows the result of simulating the marginally stable case at $\alpha=(3+3/8)\pi$. The simulation moves toward equilibrium and quickly reaches a steady oscillation of small amplitude about the equilibrium.

D. Equilibria with an external capacitor

The equilibria with external capacitance were worked out earlier, such that α, T_0, and E_0 are all functions of $\phi=\alpha T_0$. These can be plugged into (37), and (37) can then be solved numerically. Figures 15–17 show the eigenvalues θ as functions of α for several different values of C. The range of α in the plots is again from $n\pi-2$ to $n\pi+2$, although this is no longer quite the right range physically. Note that the oscillatory modes that were stable in the short circuit

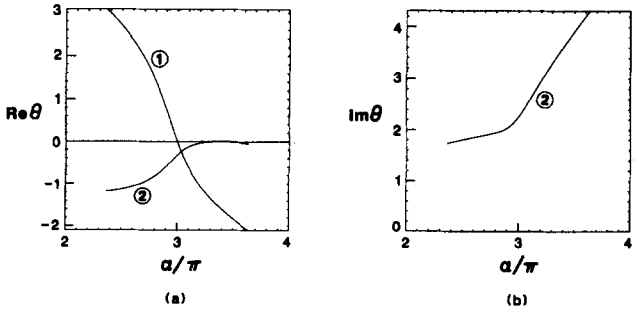

FIG. 12. Dispersion curves for dominant modes of a nonuniform equilibrium in the short circuit case for $2\pi<\alpha<4\pi$. The mode that is dominant for $\alpha/\pi<3$ is purely growing.

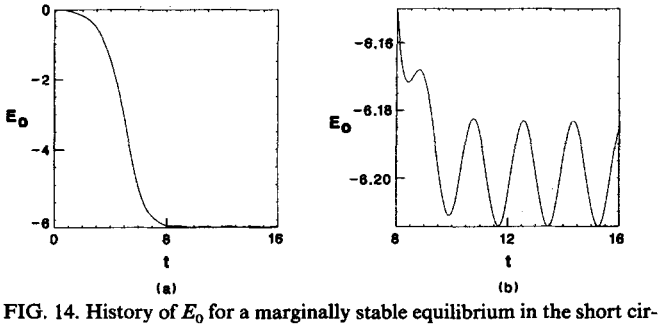

FIG. 14. History of E_0 for a marginally stable equilibrium in the short circuit case at $\alpha/\pi=3+3/8$. Figure (b) is a blowup of the last half of Fig. (a).

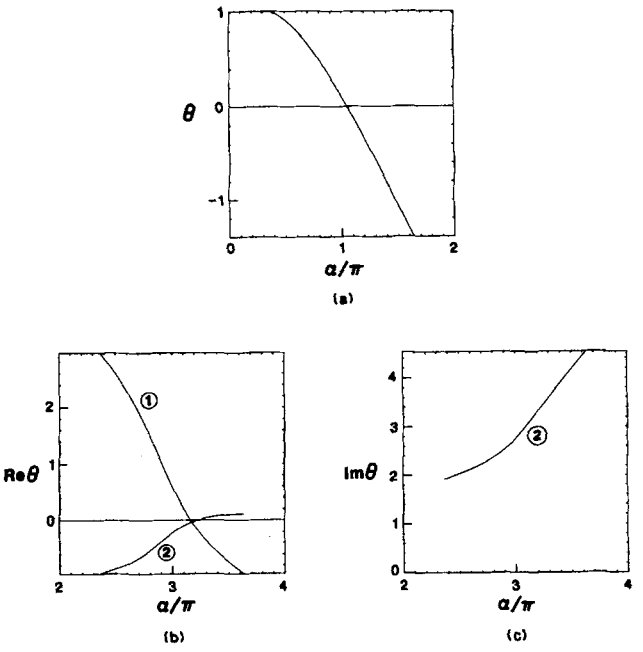

FIG. 15. Dispersion curves for dominant modes of a nonuniform equilibrium for $C = 20$. The mode which is dominant for $2 < \alpha/\pi < 3$ is purely growing.

case have become unstable for some values of α with the addition of an external capacitor, counter to the stabilizing influence of the capacitor on the modes of the uniform equilibrium. These theoretical results agree with the simulation results obtained earlier.

The newly unstable modes are the most interesting ones. A natural question is whether they saturate at some finite

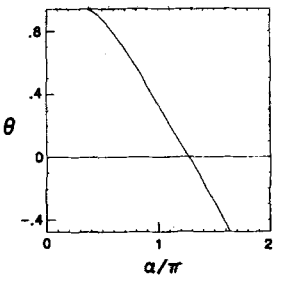

FIG. 17. Dispersion curves for dominant modes of a nonuniform equilibrium for $C = 5$.

amplitude due to nonlinear effects. Figure 18 shows that for $C = 20$, the $\alpha = 7/2\pi$ case, at least, does not. The initial transient brings the system close to the (unstable) equilibrium (at $t \sim 10$), but then the instability takes over, and grows until, finally, electrons are turned back to the injection plane. Since their charge remains on the left side of the system (and the left side of the external capacitor), the system is no longer in a state that allows the unperturbed ($E_0 = 0$, $V = 0$) equilibrium and so the resulting equilibrium (shown at $t = 64$) has not been included in my analysis of equilibria. (Such equilibria could be worked out, but require the addition of another parameter, specifically, the sum of the charge on the injection plane and the side of the capacitor tied to it.)

Once a certain amount of charge has been returned to the emission plane, the system is in an equilibrium that has a stable spectrum. Interestingly, the potential drop across the system in this new equilibrium is nearly zero. It seems unlikely that this could be coincidence, but it also seems unlikely that a gross process, such as virtual cathode formation, could return precisely the correct amount of charge for this to occur.

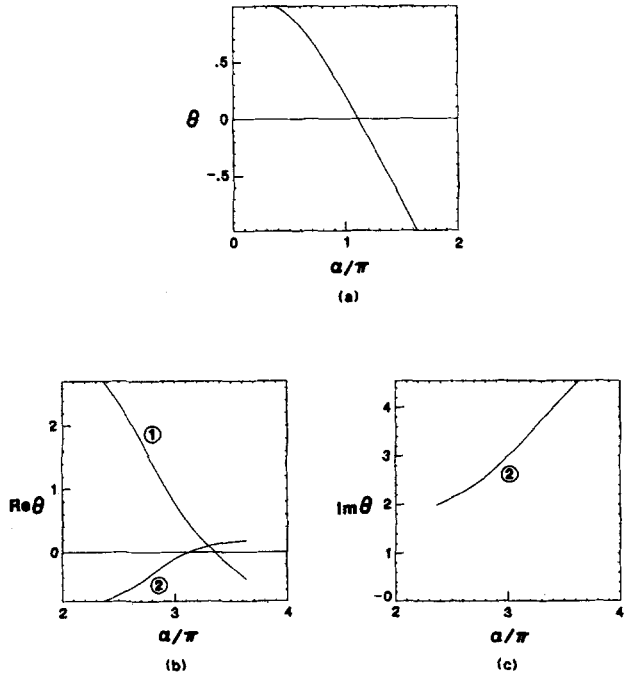

FIG. 16. Dispersion curves for dominant modes of a nonuniform equilibrium for $C = 10$. The mode which is dominant for $2 < \alpha/\pi < 3$ is purely growing.

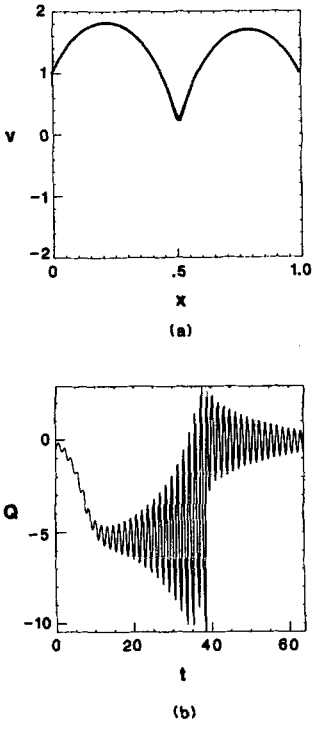

FIG. 18. Phase space at $t = 64$ and history of the charge on external capacitor Q. Between $t = 35$ and $t = 40$, electrons are turned back to the injection plane, producing a state that cannot return to the uniform equilibrium. Note there are two trapped electrons in the first half of the system.

V. CONCLUSIONS

The theory for nonuniform (nonlinear) equilibria of the Pierce diode with an external capacitor instead of a short circuit between its electrodes was worked out, and simulations were performed that verified the theory for both the capacitive Pierce diode and the classical Pierce diode.

The spectra of oscillations about nonuniform equilibria of the Pierce diode with and without an external capacitor have also been calculated, and the results are consistent with the simulation results, although the simulations were not examined to high precision.

Of particular interest is the observation that strong, regular virtual cathode oscillations can occur at current levels that are much smaller than the current level at which the Pierce diode becomes linearly unstable (simulations were performed at one quarter of this current value). As Godfrey showed, it is also possible to exceed the current level at which the Pierce diode becomes unstable by any amount desired, *if* the proper stable nonuniform equilibrium can be attained.

The effect of the external capacitor is to stabilize the linear modes somewhat, and also to increase the current value at which virtual cathode oscillations can be excited. The external capacitance has the detrimental effect, however, of limiting the maximum current that can be carried by the nonlinear modes. The most useful mode ($n = 1$) ceases to exist for values of α greater than some maximum, and the other modes tend to become unstable.

The effects of external resistance and inductance on the dispersion of the nonuniform equilibria have not been investigated.

ACKNOWLEDGMENTS

I gratefully acknowledge the valuable advice and assistance of Professor C. K. Birdsall and Dr. T. L. Crystal. The author also thanks Dr. B. Godfrey for his assistance and encouragement.

This work was performed under U.S. Department of Energy Contract DE-AT03-76ET53064 and Office of Naval Research Contract N00014-85-K-0809. The simulations were performed on the computers of the National Magnetic Fusion Energy Computer Center at the Lawrence Livermore National Laboratory.

[1] J. R. Pierce, J. Appl. Phys. **15**, 721 (1944).
[2] J. R. Cary and D. S. Lemons, J. Appl. Phys. **53**, 3303 (1982).
[3] T. L. Crystal and S. Kuhn, Phys. Fluids **28**, 2116 (1985).
[4] B. B. Godfrey, Phys. Fluids **30**, 1553 (1987).
[5] S. Kuhn and M. Hörhager, J. Appl. Phys. **60**, 1952 (1986).
[6] W. S. Lawson, Ph.D. thesis, University of California, Berkeley, 1987; W. S. Lawson, submitted to J. Appl. Phys.
[7] W. S. Lawson, J. Comput. Phys. **80**, 253 (1989).
[8] F. B. Llewelyn, *Electron Inertia Effects* (Cambridge U. P., London, 1941).

The Pierce diode with an external circuit. II. Chaotic behavior

William S. Lawson[a)]
Electronics Research Laboratory, University of California, Berkeley, California 94720

(Received 22 February 1988; accepted 28 March 1989)

The existence of the strange attractor discovered by Godfrey [Phys. Fluids **30**, 1553 (1987)] in the neighborhood of $\alpha = 3\pi$ for the Pierce diode is verified, and his numerical results are refined. The theory of Feigenbaum for the sequence of period-doubling bifurcations [J. Stat. Phys. **19**, 25 (1975)] is tested with good agreement, despite the strong assumptions made by that theory. The evolution of this attractor is then followed as an external capacitance is introduced, producing a family of bifurcation diagrams. Examination of these diagrams produces one result that should be of interest to mathematical physicists: The existence of an unstable equilibrium in the neighborhood of the strange attractor is strongly implicated in both the existence and destruction of the attractor. The reversibility of the equations of evolution is also discussed, but no clear-cut conclusion is reached.

I. INTRODUCTION

The Pierce diode is perhaps the simplest realistic theoretical model for a bounded one-dimensional plasma system. It is comprised of two parallel electrodes with electrons injected at one of the electrodes with velocity v_0. Ions are considered to be infinitely massive, forming a uniform background that neutralizes the charge density of the electrons at the electrode from which the electrons are injected. The electrodes are also held at the same potential, i.e., short circuited. This short circuit allows feedback, and leads to a wealth of interesting behavior. The Pierce diode is completely characterized by a single dimensionless parameter $\alpha = \omega_p L / v_0$, where ω_p is the plasma frequency of the electron beam and L is the distance between the electrodes.[1]

One interesting feature of the Pierce diode that was discovered by Godfrey[2] (who also investigated the nonlinear equilibria of the classical Pierce diode) is that, for a narrow range of the parameter α, the Pierce diode exhibits chaotic behavior without violent disruption (violent disruption meaning virtual cathode formation and the return of electrons to the emitter). This behavior was observed through simulations in the neighborhood of $\alpha = 2.85\pi$, and it is believed to recur approximately at intervals of 2π. The observed behavior includes a Hopf bifurcation followed by period-doubling bifurcations leading to chaotic behavior following the scenario described by Feigenbaum.[3] The reason for the formation of the observed strange attractor is uncertain, but its sudden disappearance is associated with a nearby unstable equilibrium state.

The extended Pierce diode is similar to the standard (or classical) Pierce diode, but instead of a short circuit between the bounding electrodes, a series RLC circuit is used (see Fig. 1). The behavior of the extended Pierce diode in the linear regime has been worked out by Kuhn and Hörhager[4] and verified through simulation.[5] Its nonuniform equilibria have also been investigated.[6]

In the work that follows, only an external capacitor will be introduced. The external resistance and inductance will be ignored. This might seem arbitrary, but only the external capacitance alters the equilibria of the diode, and the relationship between the strange attractor and the neighboring equilibria is of interest. Furthermore, the time and energy required for an exploration of a three-dimensional parameter space does not seem cost-effective.

First the mathematical and physical meaning of the equations will be explored, then the numerical method will be described. Once these preliminaries are out of the way, the results of Godfrey will be confirmed, although it will be found that the convergence of some of the numerical results was incomplete. The bifurcation diagram can be used to compute what should be an approximation to Feigenbaum's number, and the results are in good agreement.

When the external capacitor is introduced, it will be found that the maximum extent of the strange attractor closely follows the position of the neighboring unstable equilibrium. Circumstantial evidence will be presented for this unstable equilibrium being responsible both for the existence of the strange attractor and the destruction of the attractor basin at small enough values of α.

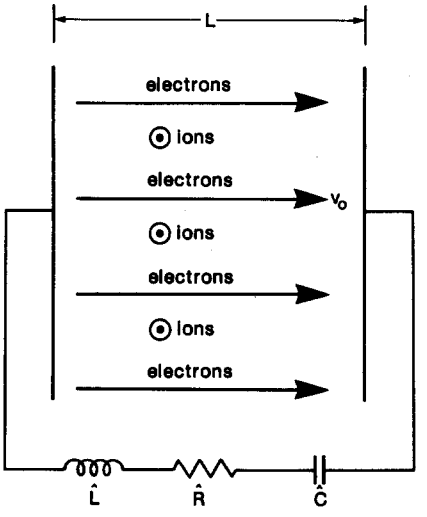

FIG. 1. Extended Pierce diode model.

[a)] Present address: Courant Institute of Mathematical Sciences, New York University, New York, NY 10012.

 0899-8221/89/071493-09$01.90

II. GENERAL PROPERTIES OF THE PIERCE DIODE EQUATIONS

The equations of evolution for the Pierce diode with an external capacitor were derived in the preceding article.[6] They are

$$T(t) = 1 - \frac{1}{\alpha}\int_{t-T}^{t} E(\tau)\sin\alpha(t-\tau)d\tau \tag{1}$$

and

$$\left(1+\frac{1}{C}\right)E(t) = \frac{\alpha^2}{2}[1-T(t)^2] - \alpha\int_{t-T}^{t} E(\tau)(t-\tau)\sin\alpha(t-\tau)d\tau, \tag{2}$$

where $T(t)$ is the transit time of the electrons just leaving at time t (normalized to the transit time of the uniform equilibrium), $E(t)$ is the electric field at the injection plane at time t (also suitably normalized), and C is the external capacitance (normalized to the vacuum capacitance between the confining plates).

The only way in which the external capacitance enters is in the factor in front of Eq. (2). This might seem like an insignificant change, but it will be seen that the solution is profoundly altered when C is changed.

These equations have several properties that are not obvious. One important property that is not yet known, is whether this equation is reversible in time; specifically, given $E(t)$ over a transit time, is $E(t)$ unique for earlier times than those given? This question is of great importance in understanding the character and origin of the strange attractor. Evidence will be presented for both sides of this question, but a definitive answer is not yet known.

The most obvious property of this equation is that it is not what is usually called an equation of evolution, since the formulas do not specify time derivatives of the variables, but rather the variables themselves. This simplifies the numerical solution of the equations, but complicates the issue of reversibility. Another fundamental property of the equations is that $T(t)$ is purely an auxiliary variable; given $E(t)$ over a long enough initial time (long enough for the electron emitted at the earliest time to have exited), $T(t)$ can be computed for any time at which it is needed.

A less obvious property of these equations is that perfectly valid initial conditions for the *physical* problem cannot always be translated into initial conditions for these equations. Consider, for example, the perfectly reasonable conditions of sinusoidally perturbed positions, and uniform velocities, i.e., $v(x) = 1$ and $x(t_0) = t - t_0 + \epsilon \sin kt$ (dimensionless variables shall be used throughout this article). The equations for x and v as functions of t and t_0 (from Ref. 6) are

$$x = t - t_0 + \frac{1}{\alpha}\int_{t_0}^{t} E(\tau)\sin\alpha(t-\tau)d\tau \tag{3}$$

and

$$v = 1 + \int_{t_0}^{t} E(\tau)\cos\alpha(t-\tau)d\tau. \tag{4}$$

If $v = 1$ for all t_0, then plainly, $E(\tau) = 0$ for all $\tau < t$. This precludes the desired perturbation in position, however. Thus this initial situation could not have come about from the evolution of the system, and the full fluid equations must be used to advance the system for one complete transit time before Godfrey's integral equations can be applied. This, in turn, would seem to imply some loss of information, and some irreversibility over at least the first transit time.

The loss of information is more obvious from the simple consideration that in choosing the initial conditions, one can choose $\rho(x)$ and $v(x)$ without constraint, whereas in choosing the initial conditions for Godfrey's equations, only one function, $E(t)$, may be chosen.

There is no strong reason to expect more loss of information after one transit time, though, since after a transit time all the electrons in the system are subject to the constraint that at their time of injection $\rho = v = 1$. This imposes a constraint between ρ and v that did not exist in the initial conditions. This constraint is enough to guarantee that ρ and v can be reconstructed from $E(t)$. This loss of information can clearly be seen in Fig. 2, which shows a potential plot for a Pierce diode that was loaded with random perturbations in position. The potential behind the last of the initially loaded particles is smooth, but the potential ahead of it is still quite noisy. To summarize, the complete fluid equations are irreversible (due to the loss of particles at uncontrolled velocity and density at the collection plane), but the integral equations, which have an additional constraint, *may* be reversible. The issue of reversibility will be brought up again when the return maps are discussed.

A. Physical validity of solution

For Eqs. (1) and (2) to be *physically* valid, it is necessary for the velocity of the stream of particles to be a single-valued function of position. The situation depicted in Fig. 3(a) is physically valid, but the integral equations do not correctly model it. Since the velocity is single-valued function of t_0, it is only necessary for x to be a monotonic (in this case decreasing) function of t_0. From Eq. (3),

$$\frac{dx}{dt_0} = -1 - \frac{1}{\alpha}E(t_0)\sin\alpha(t-t_0) < 0, \tag{5}$$

so, physically, it is necessary that

$$E(t_0)\sin\alpha(t-t_0) > -\alpha. \tag{6}$$

Since α is large, this implies that whenever

$$|E(t)| < \alpha \tag{7}$$

is violated, the solution will soon become unphysical.

Another situation that is not physically allowed but can occur in the solution of Eqs. (1) and (2) is that depicted in Fig. 3(b). Here, the velocity of the "outgoing" particles has

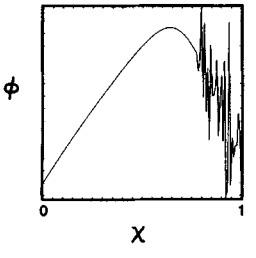

FIG. 2. Pierce diode simulation run before initially loaded particles have left the system.

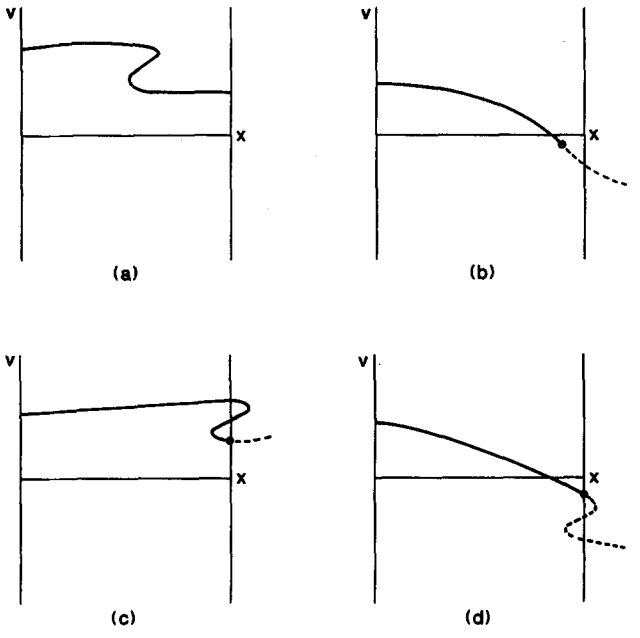

FIG. 3. Situations that limit the physical and mathematical validity of the solution. In (a), the velocity is not a single-valued function of position, in (b), particles that have left the model return; in (c) and (d), the transit time T ceases to exist.

reversed, so that particles which physically would have been absorbed (but which still exist mathematically), are reentering the region of interest. Again, the Eqs. (1) and (2) allow this without contradiction, even though the situation is unphysical. The simplest test for this situation is that when

$$\frac{dT}{dt} > 1 \tag{8}$$

the solution is no longer physically valid. The transit time T represents the "age" of whatever particle is at the exit plane. If this age is increasing faster than the flow of time, then it must be that particles which were once past the boundary are reentering.

Mathematically speaking, the physical constraints on the solution are rather arbitrary. Since the solution of Eqs. (1) and (2) may be of *mathematical* interest despite being unphysical, in the work presented here, *all purely physical restrictions have been ignored*. The situations represented in Figs. 3(a)–(d) are thus allowed, but the situations shown in Figs. 3(c) and 3(d) will eventually lead to problems of a mathematical character that dictate the termination of the solution. In Fig. 3(c), the particles in the top part of the S are affecting the solution even though they have passed beyond the physical boundary of the system, because they were emitted at a time later than $t - T$, and so are still included in both Eqs. (1) and (2). This is mathematically acceptable. The difficulty arises when the lower bend of the S moves across the right-hand boundary, and the solution for T [from Eq. (1)] ceases to exist. A new solution could be found, but it would have to jump discontinuously, and since the solution has already lost physical validity, there can be no justification for this.

In Fig. 3(d), the opposite problem occurs as in Fig. 3(c). Again, the solution for T ceases to exist, and the integration of the equations must stop. Both the situations in Fig. 3(c) and Fig. 3(d) occur when dx/dt_0 at the exit plane ($t = t_0 + T$) becomes zero. Thus, from Eq. (5), when

$$1 + (1/\alpha)E(t - T)\sin \alpha T \to 0, \tag{9}$$

the integration of the equations must end. *This is the only criterion (other than a time limit) on which the integration was stopped.*

In practice, the effect of the physical restrictions is to impose an amplitude limit on the oscillations. This has no effect on the bifurcation diagram for $C = \infty$ (the short circuit case), but as the external capacitance is decreased, the amplitude of the stable oscillations tends to increase, and so part of the high-amplitude end of the bifurcation diagram will be lost.

III. NUMERICAL INTEGRATION SCHEME

The integral equations are of nonstandard form, and the method of numerical integration used is, therefore, unusual. As with most methods of time integration, the continuous functions E and T are discretized at uniform time intervals $t_{n+1} = t_n + \Delta t$, so that $E_n \approx E(t_n)$, and similarly for T.

Inspection of Eq. (1) reveals that only the left-hand side of the equation (for $t = t_n$) depends on a quantity known at t_n, since the kernel of the integral vanishes at $\tau = t$. Thus the integral can be evaluated numerically, in order to find T_n (this is a little tricky, since the lower integration limit depends on T_n, but some simple algebra solves the problem). This value of T_n can be put into Eq. (2), and the integral in Eq. (2) can be evaluated just as the integral of Eq. (1) was, in order to calculate E_n.

There is a slight difficulty in evaluating the integrals at the lower limit of $\tau = t - T$. Since the transit time T will not be a multiple of the time step Δt, the last interval to be integrated will not be a full time step wide. This fraction of a time step need not be evaluated as accurately as the rest of the integral (since the error it produces occurs only once), but it cannot be ignored. If the trapezoidal rule is used for the integration, then linear interpolation of the indefinite integral is sufficiently accurate (some runs with a more sophisticated method of handling the last time step verified this). It is not clear that a higher-order method of integration (e.g., Simpson's rule) would improve the accuracy of the results, since the derivation of these higher-order methods assumes that the function to be integrated is a known, smooth function, whereas our integrand is a discrete approximation.

It is possible to speed up the numerical scheme considerably by expanding $\sin \alpha(t - \tau)$ and writing

$$\int E(\tau)\sin \alpha(t - \tau)d\tau = \sin \alpha t \int E(\tau)\cos \alpha\tau \, d\tau - \cos \alpha t \int E(\tau)\sin \alpha\tau \, d\tau. \tag{10}$$

The integrands on the right do not depend on time, and the limits of integration vary slowly with time. This allows the integrals to be computed each time step by adjusting for the

small change in the limits of integration rather than recomputing the entire integral. This saves much computer time. This scheme does require that α be strictly constant, which is a problem in generating bifurcation diagrams; however, α can be varied by small jumps, after which the integrals on the right-hand side of Eq. (10) must be completely reevaluated. The solution before the jump in α becomes the initial condition on the solution after the jump. If these jumps are infrequent, much computer time can still be saved by using this scheme.

This numerical integration scheme was tested on some equilibrium solutions that are known from theory,[2] and when the time step was 1/256 of a transit time, the results were accurate to four decimals. It is to be expected that the time-varying solution will be less accurate, but of the same order of accuracy.

As was mentioned in the previous section, the integration must be stopped when condition (9) occurs. Not surprisingly, the left-hand side of Eq. (9) occurs as a denominator in the equation for correcting the value of T each time step, and the method of integration fails when condition (9) occurs. Testing condition (9) is therefore quite simple.

The study of discretized integral equations like this one has only just begun. The sole instance located so far of such study barely touched on convolutions of the form of Eqs. (1) and (2), and did not include the variable interval of integration.[7]

IV. VERIFICATION OF THE RESULTS OF GODFREY

The results given by Godfrey have been confirmed in each case in which they have been tested, with one exception that does not modify the important conclusions. Figure 4 shows the bifurcation diagram obtained by Godfrey as a function of α (this is Godfrey's Fig. 10). His time step (normalized to the unperturbed transit time L/v_0) was roughly 1/50. His Poincaré section was chosen at the maximum value of $T(t)$ of each orbit. In order to make comparison of our results simpler, this same section was used in the present work, even though it is not clear that it is a truly valid Poincaré section. (Choosing the maximum of T as the Poincaré section is not necessarily valid since the locus of all points which are maxima of T for different cycles is not necessarily a continuous or well-behaved curve in E-T space.)

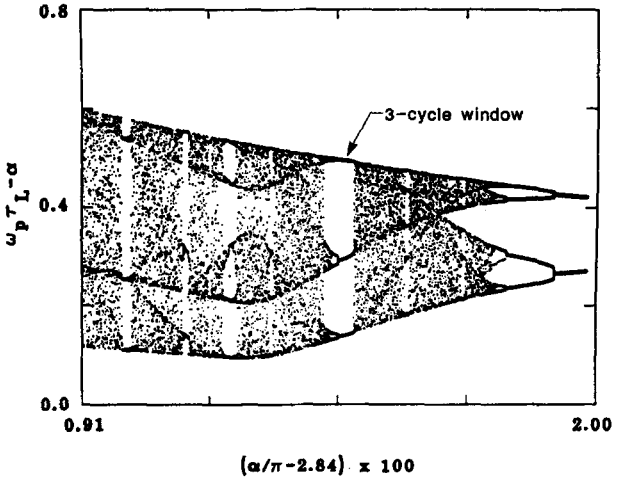

FIG. 4. Bifurcation diagram obtained by Godfrey. A 3-cycle window is indicated by the arrow. The first bifurcation is off the right side of the plot, but the second bifurcation is visible as a pair of Y's.

Godfrey's results were reproduced by using the same time step, but smaller time steps produce somewhat different results, particularly for smaller values of α. Successive halving of the time step reveals that the diagrams generated by time steps of 1/256 and 1/512 are visually indistinguishable (see Fig. 5), but quite different from the diagram generated by Godfrey. While the strange attractor remains, as well as all other important results, it is necessary to conclude that the time step in Godfrey's work was not small enough to produce the accuracy necessary for generating the correct bifurcation diagram. In all the work that follows, a time step of 1/256 is used.

One casualty of the better convergence of the bifurcation diagram is the break Godfrey observed in a period-5 window (the attractor shifted suddenly from one position to another as α was varied continuously), since the entire period-5 window is an artifact of the incomplete convergence. (A window is a range of values of α over which the motion is regular, and the period number is the number of cycles about the center of the attractor the orbit makes before closing on itself.) An even more striking jump from one chaotic attractor to another was observed, however, in the bifurcation diagram for $C = 1000$ (C being the external capacitance), as will be discussed.

One of the most important results obtained by Godfrey is that the return map (a plot of each point of the Poincaré map versus its predecessor) appears to be one dimensional, i.e., a line with no thickness or structure. If the return map is truly one dimensional, then it generates an irreversible sequence of points, i.e., knowing everything about a point tells you what its successor will be, but its predecessor may be indeterminate. To verify this result, rather than use Godfrey's Poincaré section (which carries no guarantee of being a *continuous* section, i.e., a smooth curve cutting across the trajectories in E and T space), a section is made at $T = 0$, $dT/dt < 0$. Also, consecutive values of E are plotted rather than values of T. Figure 5 is marked with the values of α for which return maps are shown in Figs. 6–10.

Figure 8, although a seemingly chaotic region of the bifurcation diagram, shows the eventual appearance of an 11 cycle after a long initial chaotic transient.

Note that although the maps are not single valued, they have no discernible structure within the line (except for one small spur on the most complex one). This implies that either the equations of motion are irreversible, or that the subdominant eigenvalue of perturbations about the chaotic orbit is *much* less than the dominant one. There is one clue that the second possibility may be the correct one in that very near the point at which the attractor ends (Fig. 10), the curve develops a spur on one of the bends in the lower right corner of the return map, which indicates that an infinitude of such spurs may exist for all values of α, but lie so close to the rest of the attractor that they cannot be seen. If this is the case, then the return map is actually of fractional dimension

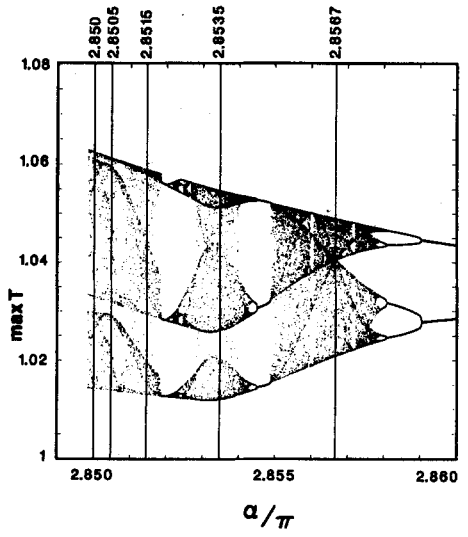

FIG. 5. Bifurcation diagram for $\Delta t = \frac{1}{256}$ (indistinguishable from the diagram for $\Delta t = \frac{1}{512}$. The vertical lines mark the values of α at which return maps will be plotted.

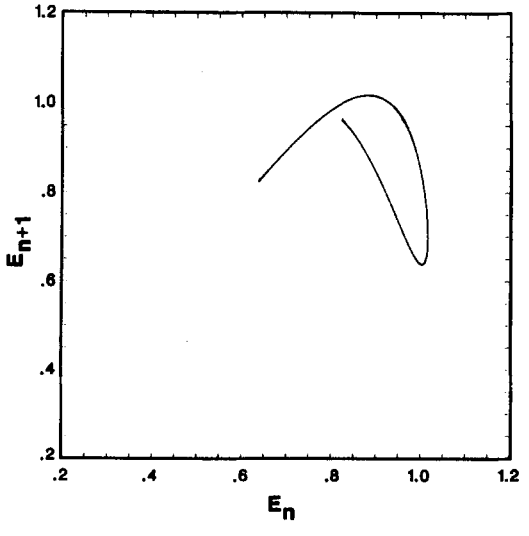

FIG. 6. Return map for $\alpha = 2.8567\pi$.

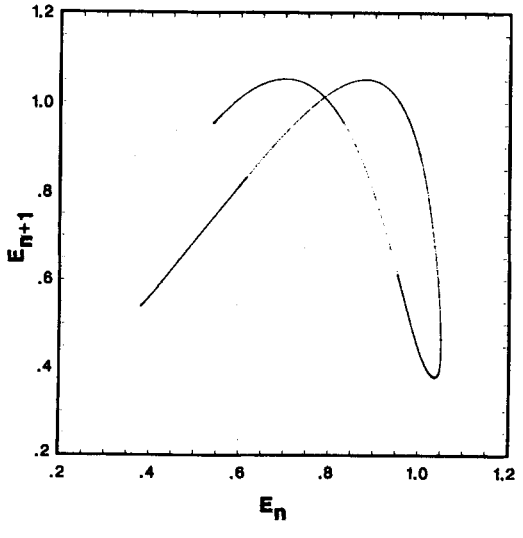

FIG. 7. Return map for $\alpha = 2.8535\pi$.

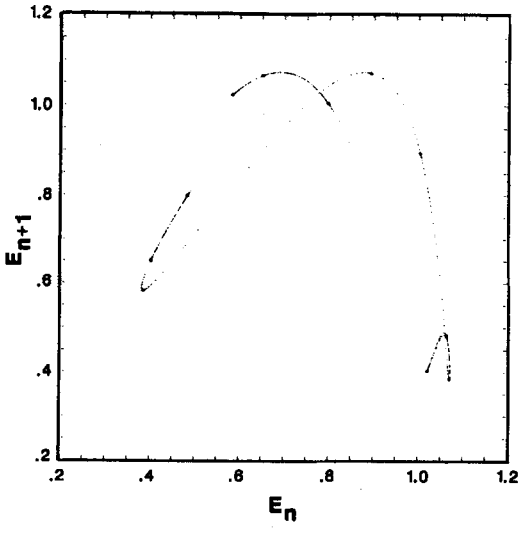

FIG. 8. Return map for $\alpha = 2.8515\pi$. Note the dots indicating a possible stable 11-cycle.

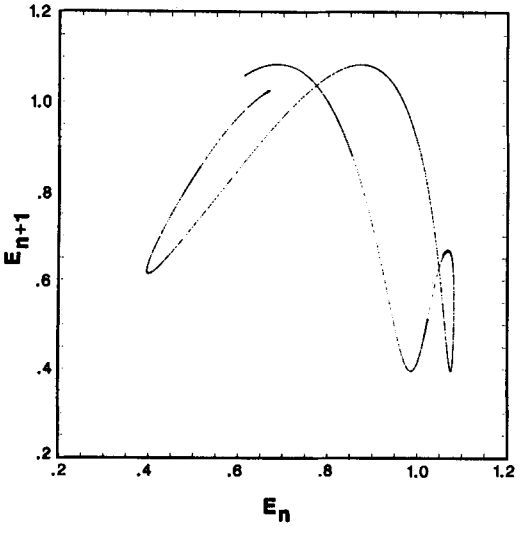

FIG. 9. Return map for $\alpha = 2.8505\pi$.

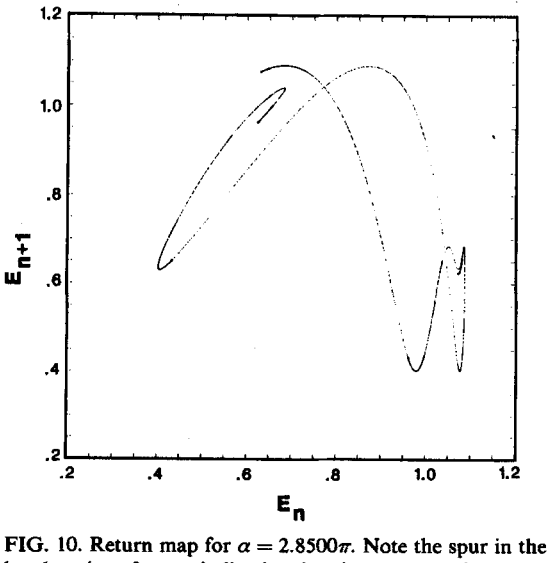

FIG. 10. Return map for $\alpha = 2.8500\pi$. Note the spur in the lower right-hand section of curve, indicating that the curve may have much unresolved structure.

(probably very close to dimension one), and the flow *could* then be completely time reversible.

The second, third, and fourth period-doubling bifurcations can be used to find an approximation to what one would expect to be Feigenbaum's number.[3] The values of α at these points are $\alpha_1 = 2.858\ 109\ 0 \pm 0.000\ 000\ 5$, $\alpha_2 = 2.857\ 891\ 2 \pm 0.000\ 000\ 2$, and $\alpha_3 = 2.857\ 844\ 2 \pm 0.000\ 000\ 1$, from which the value $(\alpha_1 - \alpha_2)/(\alpha_2 - \alpha_3) = 4.63 \pm 0.03$, which is in fairly good agreement with Feigenbaum's number 4.669.

An interesting, and to my knowledge unreported, phenomenon is noticeable in these bifurcation diagrams. A pattern of short vertical lines seems to follow a straight horizontal line from the last band merging (at $\alpha = 2.856\ 71\pi$) on. Fainter patterns can be seen starting from other band mergings. This effect can be seen better in a blowup of the region of the last band merging (see Fig. 11). The effect is also observable in bifurcation diagrams derived from one-dimensional noninvertible maps (see Ref. 8). This apparent structure is due to the presence of an unstable cycle. The system orbit is not likely to pass near this unstable cycle, but when it does, it tends to stay near it for a longer time, since both the approach and retreat are exponential (just as a ball rolling up and over a hill will spend most of its time near the top). Thus, since only a limited number of orbits are completed for each value of α, some values of α will show no points near the unstable cycle, and others will show many. On the average, the density of points is neither enhanced nor depleted at these unstable cycles.

Godfrey also commented on the destruction of the strange attractor resulting from the collision of the attractor with an unstable equilibrium, a situation called a crisis.[9] Discussion of this phenomenon will be deferred until the results for finite values of the external capacitor have been described, since they add much to the evidence.

V. STRANGE ATTRACTOR WITH AN EXTERNAL CAPACITOR

Before examining the behavior of the strange attractor as the capacitance is varied, it is important to examine the linear and equilibrium characteristics of this region as a function of the capacitance. The real part of the growth rate is shown as a function of α for several values of the capacitance in Fig. 12. Note that for infinite capacitance, the growth rate is zero for $\alpha = 2\pi$, and negative for a short region of α just less than 3π. With the introduction of a large external capacitance, the growth rate at 2π becomes negative (the transition from negative to positive, at α slightly larger than 2π, also becomes a Hopf bifurcation), and the growth rates near $\alpha = 3\pi$ become *less* negative. This trend continues until the external capacitance $C = 8$, at which point the growth rate at $\alpha = 3\pi$ becomes exactly zero (as can be shown from the dispersion relation). At $C = 8$, the growth rate is entirely non-negative near $\alpha = 3\pi$. The growth rate for $\alpha = 3\pi$ peaks at $C = 8$, so for $C < 8$, it once again becomes negative near $\alpha = 3\pi$. As C becomes smaller, the growth rate is positive for a narrower and narrower range of α, until at roughly $C = 4$, the system is linearly stable for all $2\pi < \alpha < 3\pi$.

The unstable equilibrium, which is responsible for the crisis that terminates the strange attractor, is a sensitive function of C. Figure 13 shows the value of E_0 at the unstable equilibrium versus α for several values of C. The equilibrium ceases to exist physically for $E_0 < -\alpha$, but is still present mathematically and may still have an effect on the trajectory of the solution. The equilibrium values of T tend to increase as C is decreased.

Now let us examine how the attractor changes with the external capacitance. First the changes will simply be described, then some interpretations will be offered.

The shape of the bifurcation diagram changes rapidly

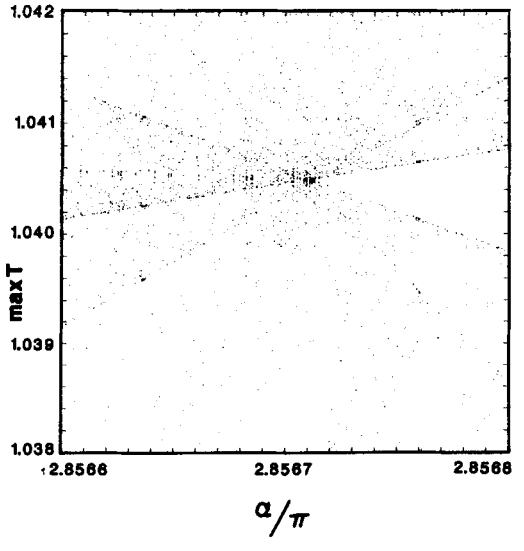

FIG. 11. Blowup of the bifurcation diagram near last band merging, showing the effect of the unstable equilibrium.

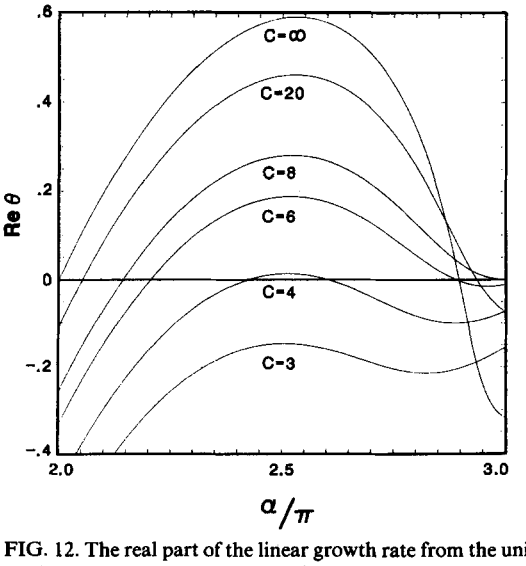

FIG. 12. The real part of the linear growth rate from the uniform equilibrium between $\alpha = 2\pi$ and $\alpha = 3\pi$ for several values of the external capacitance C.

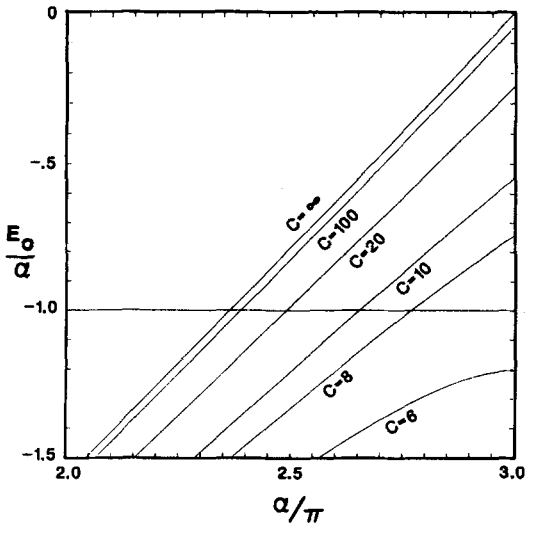

FIG. 13. Values of E_0 at the unstable equilibrium as a function of α for several values of the external capacitance C.

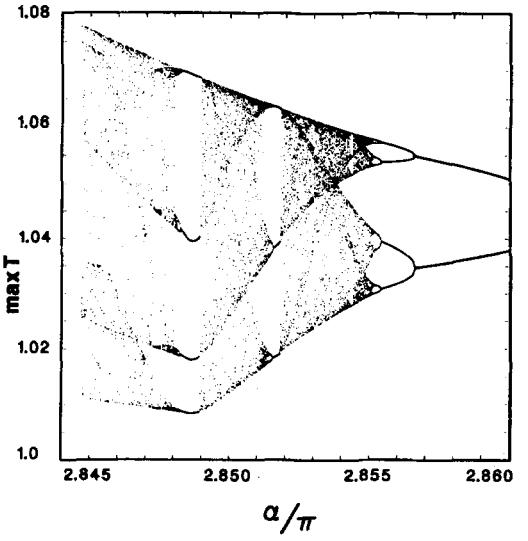

FIG. 15. Bifurcation diagram for $C = 100$.

with even rather large values of C. Figure 14 shows the bifurcation diagram for $C = 1000$, and already the shape is much altered (compare Fig. 5). This bifurcation diagram shows an interesting jump in the attractor at $\alpha = 2.8515\pi$. Both attractors appear to be chaotic, but the solution jumps suddenly from one to the other.

Figures 15–17 show the bifurcation diagrams for $C = 100$, $C = 20$, and $C = 11$, respectively. One obvious trend is that as the capacitance is decreased, the amplitude at which the crisis occurs increases, roughly in proportion to the (unstable) equilibrium value of the electric field. Between $C = 11$ and $C = 10$, the strange attractor rapidly disappears, the chaotic region disappearing first, and pitchfork bifurcations thereafter. The bifurcation diagram for $C = 10$ shows no bifurcations aside from the initial Hopf bifurcation.

While the strange attractor has vanished, the behavior for values of C less than 10 is interesting. Between $C = 9$ and,

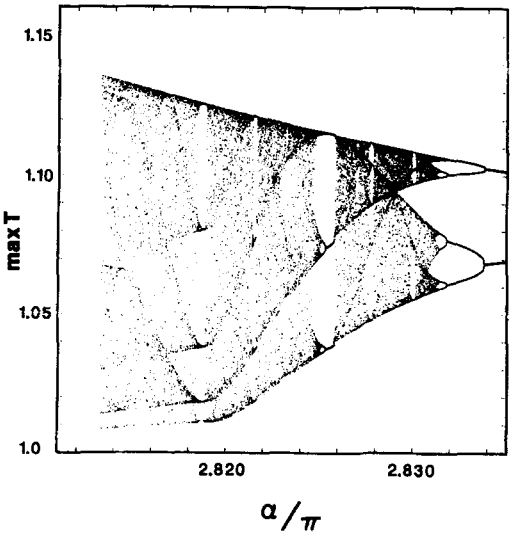

FIG. 16. Bifurcation diagram for $C = 20$.

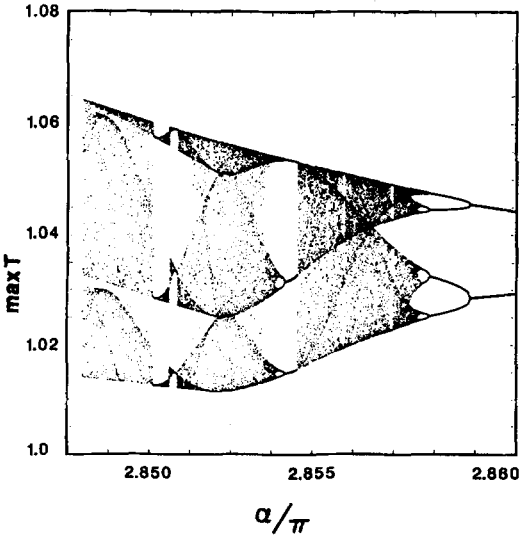

FIG. 14. Bifurcation diagram for $C = 1000$.

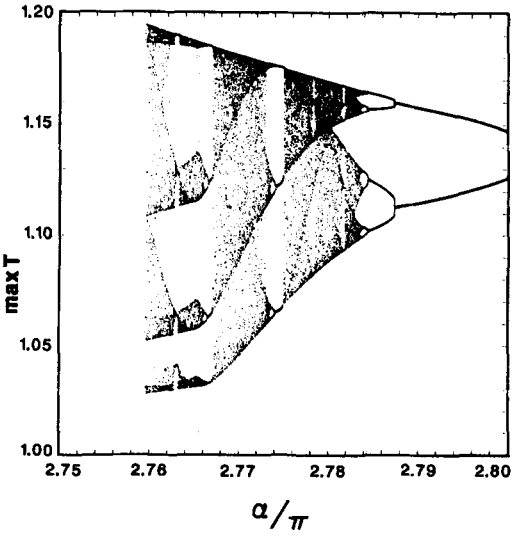

FIG. 17. Bifurcation diagram for $C = 11$.

roughly, $C = 6$, the stable limit cycle seems to cease to exist. In fact, it probably is just stable over a very narrow range of values of α, with the possible exception of $C = 8$, which has no Hopf bifurcation [the real part of the growth rate is never negative, and a double root (both roots being zero) exists at $\alpha = 3\pi$].

In the meantime, the solution for smaller α (the point of zero linear growth near $\alpha = 2\pi$ is a Hopf bifurcation for all finite values of C) becomes stable over a wider and wider range of α as C is decreased. At no time, however, does this other stable limit cycle show signs of bifurcations or chaotic behavior. At roughly $C = 5$, this limit cycle meets the limit cycle originating at higher α, forming one continuous limit cycle as a function of α. At roughly $C = 4$, the most unstable growth rate becomes zero, and only the uniform equilibrium is stable for all α between 2π and 3π.

Returning now to the strange attractor, Fig. 18 shows the orbit in E and T of the solution for $C = 11$ near the crisis ($\alpha = 2.758\pi$). The unstable equilibrium is marked as a large dot (not to be confused with the large blob at $E = 0$, $T = 1$). Just as in the $C = \infty$ case, the unstable equilibrium is clearly disturbing the attractor to a degree that it may create a hole in the attractor basin.

The shape of this orbit is rather complex, and it can be seen that one orbit does not even cross $T = 1$, creating a minor problem with the validity of the Poincaré section used for the bifurcation diagrams.

Now some general comments comparing the crisis observed in the Pierce diode and the crises studied by Grebogi *et al.*[9] are in order. Grebogi *et al.* studied noninvertible maps with one variable whose return map was known as a function of some parameter. It is possible that the Pierce diode attractor can be reduced to such a map, and it can almost certainly be reduced to a similar problem that is a noninvertible, one-dimensional map.[10] If this can be done, E is almost certainly not the best variable to use. A change is in order, but the proper variable, one which contains all the relevant information and no extraneous information, has not been found. This variable, if it exists, would produce a simple, roughly parabolic return map, as has been studied by Ott and Grebogi, and it is to be hoped that its value at the uniform equilibrium would exactly coincide with the crisis.

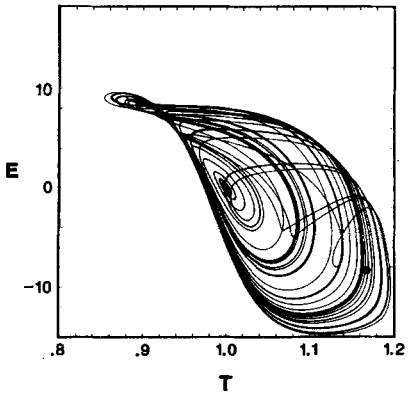

FIG. 18. Orbit trace for $\alpha = 2.758\pi$ and $C = 11$, which is just above the crisis value of α.

In the cases studied by Ott and Grebogi, the strange attractor ceased to exist only when the unstable cycle exactly contacted the attractor. It is this predictive power that makes the concept so powerful. Here, though, only the existence of the unstable equilibrium is known, and the destruction of the attractor, while clearly associated with the unstable equilbrium, cannot be predicted with any accuracy. Plainly, there is more of importance to the system at any given time than E and T at that time, since these values pass over and around the equilibrium values without creating any large disruption. Only when the value of E remains near the equilibrium value for a longer period of time does the equilibrium seem to greatly influence the solution.

An interesting question is whether the unstable equilibrium is necessary for the *formation* of the strange attractor. The lack of any strange attractor in the region just above $\alpha = 2\pi$ for any value of C is suggestive of this, since the unstable equilibrium for this region is far away from the solution. Also suggestive is the way in which the amplitude of the chaotic solutions seems to follow the value of the electric field at the unstable equilibrium.

Another indication of the importance of the unstable equilibrium in the existence of the strange attractor is the character of the orbits. The orbits seem regular, and seldom cross just before they encounter the unstable equilibrium ($T < 1$ and $E < 0$), but as they pass near it, they diverge, and, immediately afterward, they reconverge, crossing in the process. This seems to indicate that the unstable equilibrium is responsible for the exponential divergence of neighboring orbits required for a strange attractor, and that without it (if such an idea is meaningful) the orbits would quickly either converge to a steady (oscillatory) state or diverge.

VI. SUMMARY

The work of Godfrey on the Pierce diode strange attractor has been verified (with one minor correction). The strange attractor was found where expected, and followed the prediction of Feigenbaum regarding the cascade of bifurcations leading to chaos. Only the detailed structure was found to differ from Godfrey's result, this being attributed to insufficiently small time steps in Godfrey's numerical integration of the equations.

The strange attractor was studied as an external capacitance was introduced and varied, and the results were discussed. In particular, it was suggested, on the basis of circumstantial evidence, that the unstable equilibrium is necessary not only for the destruction of the attractor (in a crisis), but for the existence of the strange attractor.

ACKNOWLEDGMENTS

I gratefully acknowledge the advice and assistance of Dr. B. B. Godfrey and Professor M. A. Lieberman, and the support of Professor C. K. Birdsall.

This work was supported by U.S. Department of Energy Contract number DE-AT03-76ET53064 and Office of Naval Research Contract number N00014-85-K-0809.

[1]J. R. Pierce, J. Appl. Phys. **15**, 721 (1944).
[2]B. B. Godfrey, Phys. Fluids **30**, 1553 (1987).
[3]M. J. Feigenbaum, J. Stat. Phys. **19**, 25 (1978).
[4]S. Kuhn and M. Hörhager, J. Appl. Phys. **60**, 1952 (1986).
[5]W. S. Lawson, Ph.D. thesis, University of California, Berkeley, 1987; W. S. Lawson, submitted to J. Appl. Phys.
[6]W. S. Lawson, Phys. Fluids B **1**, 1483 (1989).
[7]A. Fulinski and A. S. Kleczkowski, Phys. Scr. **35**, 119 (1987).
[8]A. J. Lichtenberg and M. A. Lieberman, *Regular and Stochastic Motion* (Springer, New York, 1983), p. 418.
[9]C. Grebogi, E. Ott, and J. A. Yorke, Physica D **7**, 181 (1983).
[10]E. Ott, Rev. Mod. Phys. **53**, 655 (1981).